

January 10, 2019

Mr. Larry J. Gremminger  
Sunoco Logistics, L.P.  
535 Fritztown Road  
Sinking Spring, PA 19608

RE: Geophysical Survey  
Sunoco Pipeline, L.P. Pipeline Project  
Horizontal Directional Drill S2-0247 – Highway 15  
PA-CU-0176.0019-RD-16  
Upper Allen Township, Cumberland County, Pennsylvania  
RETTEW Project No. 096302009

Dear Mr. Gremminger:

RETTEW Associates, Inc. completed a multi-technique geophysical survey at the S2-0247, Highway 15 horizontal directional drill (HDD) location. The purpose of the survey was to detect and delineate subsurface voids or low-density zones beneath three portions of an HDD path that could increase the risk of inadvertent returns (IRs) and/or a loss of returns, and to determine the rock profile and rock rippability for ease-of-excavation. The following report, figures, and attachments describe the methods and results of the investigation.

### **EXECUTIVE SUMMARY**

The multi-technique geophysical survey was completed between November 12 and November 20, 2018. Four different geophysical techniques were utilized to detect and delineate subsurface voids or low-density zones and provide a rock profile. These methods, and their general results are as follows:

- Microgravity delineated low-density zones throughout the three survey areas. These zones could represent minor karst-related air-, water-, or mud-filled voids, or locally deeper rock/thicker soils.
- Seismic refraction confirmed the presence of an irregular bedrock surface or “epikarst” zone.
- Multi-Spectral Analysis of Surface Waves (MASW) identified low-velocity zones above (soft soils) and below (possible voids) the bedrock surface.
- Electrical Resistivity Imaging (ERI) identified conductive features which could represent fractures or wet soils in each of the three areas.

Results from the geophysical techniques are consistent with each other, and with the geology as mapped by the PA Geological Survey, all suggesting that the local bedrock (limestone) is karstified, with potential concentrations of dissolution cavities (of various sizes) indicated by the geophysical anomalies. In the limestone, the top-of-rock is expected to be pinnacled (highly irregular) with interfingering competent rock and residual clay soil as well as potential bedrock voids.

Engineers

Environmental  
Consultants

Surveyors

Landscape  
Architects

Safety  
Consultants

Geophysicists



## SITE DESCRIPTION

The Highway 15 HDD is located parallel to and just north of the PA Turnpike (I-76), at the I-15 Exit, in Upper Allen Township, Cumberland County, Pennsylvania (see **Figure 1**). A geophysical survey was conducted over accessible lengths of the HDD alignment and encompassed a width of roughly 20 feet (**Figure 2**). Surface conditions as well as the active roadways prohibited full access to the HDD alignment.

The site bedrock geology is karstified and consists of the Ordovician-aged Rockdale Run Formation (Orr) which is predominantly limestone with some dolomite interbeds (Berg, et al., 1980). **Figure 2** shows the mapped contact of the Rockdale Run Formation and Hamburg sequence rocks south of the HDD (Ibid.).

## KARST TERRANE

Pinnacled bedrock, closed depressions, and sinkholes are geologic features characteristic of karst terranes — i.e. terranes underlain by soluble carbonate (limestone or dolomite) bedrock in wet climates. In karst terranes, infiltrating precipitation dissolves the carbonate bedrock surface, causing the top-of-rock to retreat downward leaving behind a soil mantle composed of the insoluble clay and/or silica particles formerly bonded in the rock. Within the bedrock, percolating water enlarges fractures, bedding planes, etc. to produce solution openings ranging in size from minor seams to scenic caverns.

The main difference between a sinkhole and a closed depression is that a sinkhole may appear suddenly as a break in the ground surface (revealing a hole), whereas a closed depression typically subsides slowly with no break at the surface. The Pennsylvania Geological Survey (PA DCNR Interactive Map, 2017) records several surface depressions in the vicinity of the survey area (see black dots, **Figure 2**), and many more within a half-mile radius of the site; all within the Rockdale Run Formation (Ibid., see upper right inset to **Figure 2**).

Sinkholes form where particularly enhanced infiltration into a sufficiently-wide solution opening (often called a throat or chimney) washes the soil mantle down into cavities in the underlying rock — a process commonly called soil piping. In areas where the residual soil mantle is clay-rich and cohesive, incipient sinkholes may not display any surficial topographic expression, and are present only as air-, water-, or mud-filled voids which may grow or “stope” upwards. Eventually, the overlying soil arch may collapse under its own weight, or under the weight of an overlying structure or passing vehicle. The resulting collapse feature, or “sinkhole,” is commonly filled with the remains of the soil arch and may display rock at its base. In some cases, surficial subsidence may keep pace with soil piping at depth such that a sinkhole forms by progressive deepening of a surficial depression (sometimes called a subsidence sink), rather than by catastrophic collapse of a stoping void. **Appendix A** depicts this process.

## MICROGRAVITY SURVEY

Microgravity meters measure very small variations in gravity. Several factors can locally affect the acceleration of gravity. One factor is the local density of the bedrock or soils beneath the meter. Gravity highs (mass excesses) commonly represent locally shallow bedrock pinnacles or float blocks in the soil profile or zones of particularly massive bedrock. Gravity lows (mass deficiencies) may represent locally deep bedrock cutters, or clay seams where soil displaces bedrock; air-, water- or mud-filled voids within bedrock; stoping voids in the soil above bedrock; or zones where soils have been made less dense by removal of fines.

The residual microgravity data for this survey are shown on **Figure 3**. The values depict the general

plan-view shallow mass distribution beneath the three accessible survey areas. Lower values (red) represent local mass deficiencies or gravity lows (air- or clay-filled voids or deeper soils). Higher values (blue) represent local mass excesses or gravity highs (bedrock pinnacles or float blocks). Specific microgravity survey parameters are listed in **Appendix B**.

## SEISMIC MASW AND REFRACTION SURVEY

Seismic Refraction and MASW methods utilize the speed of seismic waves through various geologic layers and features to characterize subsurface geologic conditions. The methods enable determination of the general material types, and the approximate depth to bedrock and bedrock profile. MASW can detect low-velocity zones in soils that might represent developing sinkholes, or low velocities below the top of rock that might be associated with karst solution features or fractures. The principles of Seismic Refraction are summarized in **Appendix C**.

The seismic survey consisted of three profiles along the HDD center line (see blue triangles, **Figure 2**). Color-contour velocity models of the seismic profiles for the seismic refraction and MASW are presented on **Figures 4** and **5**, respectively. On each, the vertical scale represents relative elevation in feet, and the horizontal axis represents an along-profile distance in feet. The color contours represent average seismic velocity variations (compressional- (P-)wave velocities for refraction, and shear- (S-)wave velocities for MASW), with increasing velocities from blue to green to yellow to orange to brown (refraction, **Figure 4**), and purple to grey to tan to brown (MASW, **Figure 5**). Please note that velocity data along the first and last fifteen feet of any profile have higher uncertainty. Specific seismic refraction and MASW survey parameters are listed in **Appendix B**.

## ERI SURVEY

Electrical resistivity measurements involve driving an electrical current in the ground using two electrodes at the ground surface. The apparent resistivity of the subsurface is determined by measuring the potential difference, or voltage, between two potential electrodes with a known separation and position/orientation relative to the current electrodes. The depth and volume of the subsurface zone represented by the measured apparent resistivity is a function of the geometry of the current and potential electrodes. Apparent resistivities are converted to model or true resistivities by performing a joint inversion of all the measured apparent resistivities along a profile.

The resistivity survey consisted of nine profiles; three in each of the accessible areas, all of them parallel to the HDD center line (see orange dotted lines, **Figure 2**). The apparent resistivity data were mathematically inverted using EarthImager2D by AGI to provide a cross-sectional image of each individual profile. These are shown in **Figure 6**. Specific ERI survey parameters are listed in **Appendix B**.

## RESULTS

The microgravity data are depicted on **Figure 3** as color contours representing the relative density of the subsurface, with blue for high-density, green for “site normal”, and red for locally low-density areas. The microgravity results delineated low-mass (low-density) areas across the survey grids. This is consistent with either dissolution cavities within rock, or an irregular top-of-rock surface.

The seismic refraction data are presented as cross-sectional profiles on **Figure 4**, which indicate a general three-layer stratigraphy consisting of residual soil mantle, epikarst (or weathered rock interfingering with soil), and competent bedrock. The uppermost layer has average P-wave velocities generally less than

5,000 feet per second (fps) with a thickness of approximately 5-10 feet. This is consistent with the surficial residual clay soil mantle (shaded blue to green). The deepest layers have velocities over 10,000 fps (shaded orange to red) consistent with competent bedrock (Carmichael, R. S., 1989). The zone between roughly the 5,000 and 10,000 fps contours is commonly referred to as the “epikarst” in carbonate rock and is not really a “layer” in the stratigraphic sense. Instead, it contains soil interfingered with rock pinnacles and/or float material. In non-carbonate rock, this zone (if present) is commonly weathered rock with a gradation in properties from soil downwards to competent rock.

The MASW seismic models are presented on **Figure 5**. The MASW velocity model shows velocity changes within the bedrock layer across the profiles, and possible near-vertical low-velocity anomalies of the type commonly associated with significant fractures.

The seismic velocity models from the ray-tracing method (not shown) were compared to standard ripping charts (see **Appendix D**, Caterpillar, Inc., 1995) using the inferred/assumed layer compositions to determine the general rippability of each stratum. In general, the surficial layer down to about the top of the inferred epikarst layer (wavy dashed contour) should be readily to marginally rippable with a D9 multi-or single-shank ripper doing open field ripping, based on a weighted average velocity of about less than 5,000 fps. Below the 5,000-fps contour, ripping will get more difficult with depth, with the transition zone expected to become non-rippable below the 10,000 fps contours (based on the average ray-trace velocity of over 10,000 fps and Caterpillar charts). In carbonates, the transition zone is likely to contain competent rock pinnacles or ridges, and float blocks which may require blasting or hydraulic breaking if excavated (see **Appendix B**). The 5,000-fps contour represents the top of the epikarst/weathered rock (average inferred bedrock surface) and not the actual, likely pinnacled or irregular, surface which is often non-resolvable in karst terranes. Below the solid contour, the basal half-space has a weighted average layer velocity of over 10,000 fps based on the ray-tracing model (not shown) and is well into the non-rippable range. For trenching (as opposed to open field ripping), material **above** the 5,000-fps contour line (as low as 3,500 fps) may become non-rippable (for a CAT-330 tracked excavator or equivalent) as well. The selection of the velocity cut-off for trenching is based on correlations between the ray-tracing models (not shown), material properties, and various excavation strategies investigated by Kirsten (1982). The Limitations section contains additional important information regarding rippability estimation by seismic and other means.

The electrical resistivity results are shown in **Figure 6** as nine cross-sectional profiles, with three over each of the three accessible areas. The electrical profiles show a general two-layer model with a conductive upper layer over a more resistive lower layer, indicative of moist, conductive unconsolidated material over more resistive low-porosity bedrock. The upper layer is laterally variable, which could represent possible near-surface soil disturbances given the site development history. Deep conductive anomalies may represent dissolution features within the bedrock. In general, deep blue and purple shading (low resistivity) should represent damp soil or fill near the ground surface, and mud-filled voids or fractures below the bedrock surface. Green, yellow, orange and brown shading (higher resistivity) should represent non-porous rock.

## CONCLUSIONS

In general, the geophysical survey results display anomalies indicative of a karstified terrane with potential for IR at each of the three accessible areas of the HDD. **Figure 7** highlights the areas of concern in each of the three accessible areas. Unsurveyed (inaccessible) areas are expected to be similar. The microgravity data show only mass deficiencies, while the seismic data and ERI show both an irregular inferred bedrock

surface and anomalous low-velocity and low-resistivity features consistent with dissolution features within each of the three surveyed areas. If pipeline installation involves open trenching, and rock removal is required, blasting is not recommended since this can produce overshot cracks that provide pathways for soil piping into deeper underlying solution cavities. Once pipeline installation is complete (by any method), since subsidence in karst terranes is driven by infiltrating water, site grading and stormwater control will be key to preventing future subsidence.

## LIMITATIONS

The survey described above was completed using standard and/or routinely accepted practices of the geophysical industry, and the equipment employed represents, in RETTEW's professional opinion, the best available technology. RETTEW does not accept responsibility for survey limitations due to inherent technological limitations or unforeseen site-specific conditions. We will notify you of such limitations or conditions, when they are identifiable.

The survey is based on observation of current subsurface conditions. Therefore, while the results of this survey can be used to guide further investigations, RETTEW cannot make any warranties concerning future sinkhole occurrence — particularly under the influence of altered surface and subsurface drainage patterns due to grading and construction activities.

Rippability, while historically closely-correlated with seismic P-wave velocity, also depends on geotechnical properties of the material, on the specific method of excavation, and on the variety and size of equipment employed. For mechanical excavation, the teeth or other cutting elements must be forced into discontinuities of competent rock masses, or penetrate the fabric of weak rocks. Thus, joint or fracture spacing, aperture, and infilling will all play a role in determining whether existing discontinuities in apparently-competent rock masses can allow mechanical excavation. The strength of the intact rock will also control whether fresh discontinuities can be induced during excavation activities. Therefore, while seismic data can provide reliable guidelines, RETTEW recommends that the rocks to be excavated be checked for these other geotechnical characteristics through examination of local outcrops, test pits, or boring logs.

We have enjoyed and appreciated the opportunity to have worked with you. If you have any questions, please do not hesitate to contact the undersigned.



Charles H. Rhine, MSc, PG  
Senior Project Manager



Timothy D. Bechtel, PhD, PG  
Senior Project Manager



Felicia Kegel Bechtel, MSc, PG  
Director of Geophysics

### Enclosures

Figure 1: Topographic Basemap  
Figure 2: Data Coverage Map and Geologic Setting  
Figure 3: Residual Microgravity Results  
Figure 4: Seismic Refraction Survey Results  
Figure 5: Seismic MASW Survey Results  
Figure 6: Electrical Resistivity Survey Results  
Figure 7: Geophysical Results Summary  
Appendix A: Schematic Karst Processes  
Appendix B: Geophysical Survey Parameters  
Appendix C: Introduction to Seismic Refraction  
Appendix D: Caterpillar Ripping Charts

### References

Berg, T.M., Edmunds, W.E., Geyer, A.R., and others, 1980, Geologic Map of Pennsylvania, PA Geological Survey, 4th series.

Carmichael, R. S. (1989), Physical Properties of Rocks and Minerals, CRC Press.

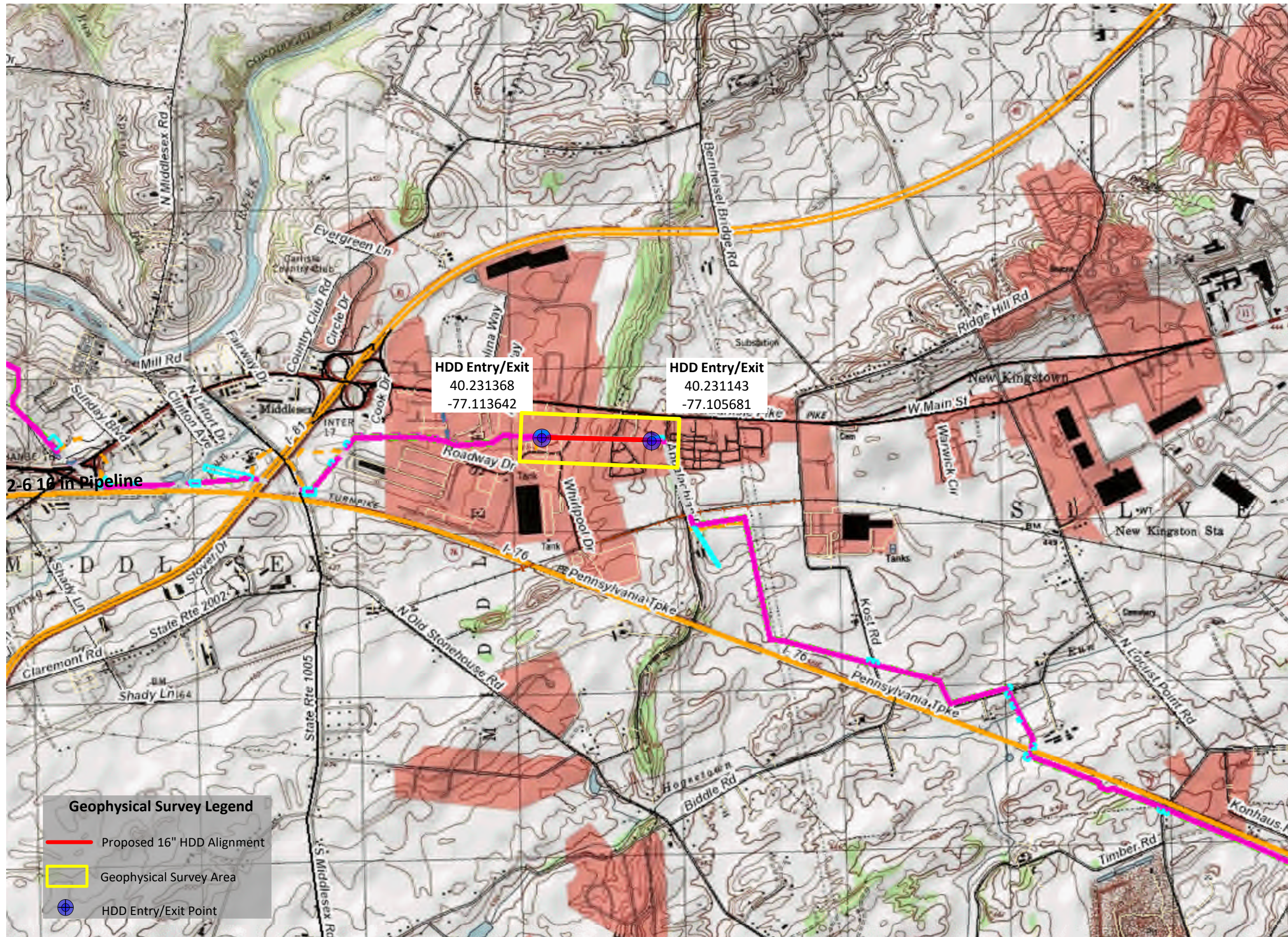
Caterpillar Tractor Company (1995), The Applicator, Caterpillar Tractor Company Marketing Division.

Kirsten, HAD (1982). A classification system for excavating in natural materials. Civil Engineering (Siviele Ingenieurswese), 24(7), 293-308.

PA Department of Conservation and Natural Resources Geology Interactive Map, (<http://www.gis.dcnr.state.pa.us.html>), 2017.

Z:\Shared\Projects\09630\096302009 - Spread 4\GP\S2-0247 Highway 15\Report\Final\HWY 15 Final Geophysic Report 2019-01-10.docx

**ENCLOSURES**



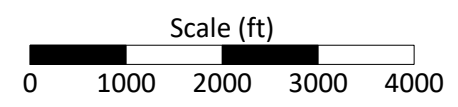
**Geophysical Survey Legend**

- Proposed 16" HDD Alignment
- Geophysical Survey Area
- ⊕ HDD Entry/Exit Point

HDD Entry/Exit  
40.231368  
-77.113642

HDD Entry/Exit  
40.231143  
-77.105681

2-6 10 in Pipeline



Notes:  
Basemap from TetraTech Sunoco Site, extracted 11/2018.

**Figure 1: Topographic Basemap**

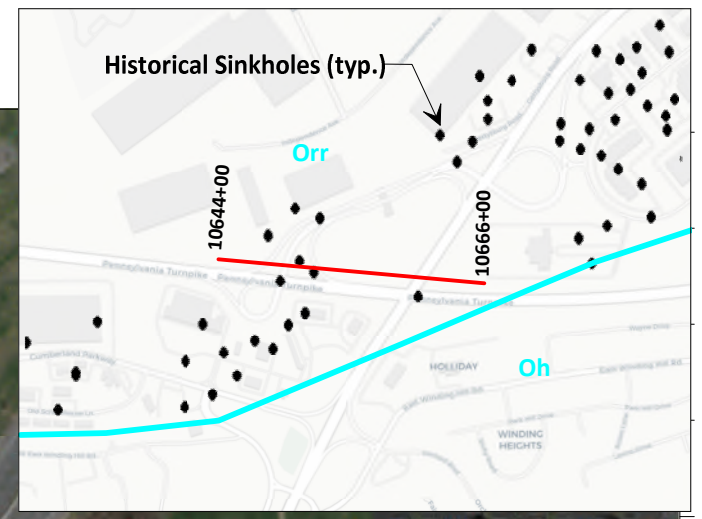
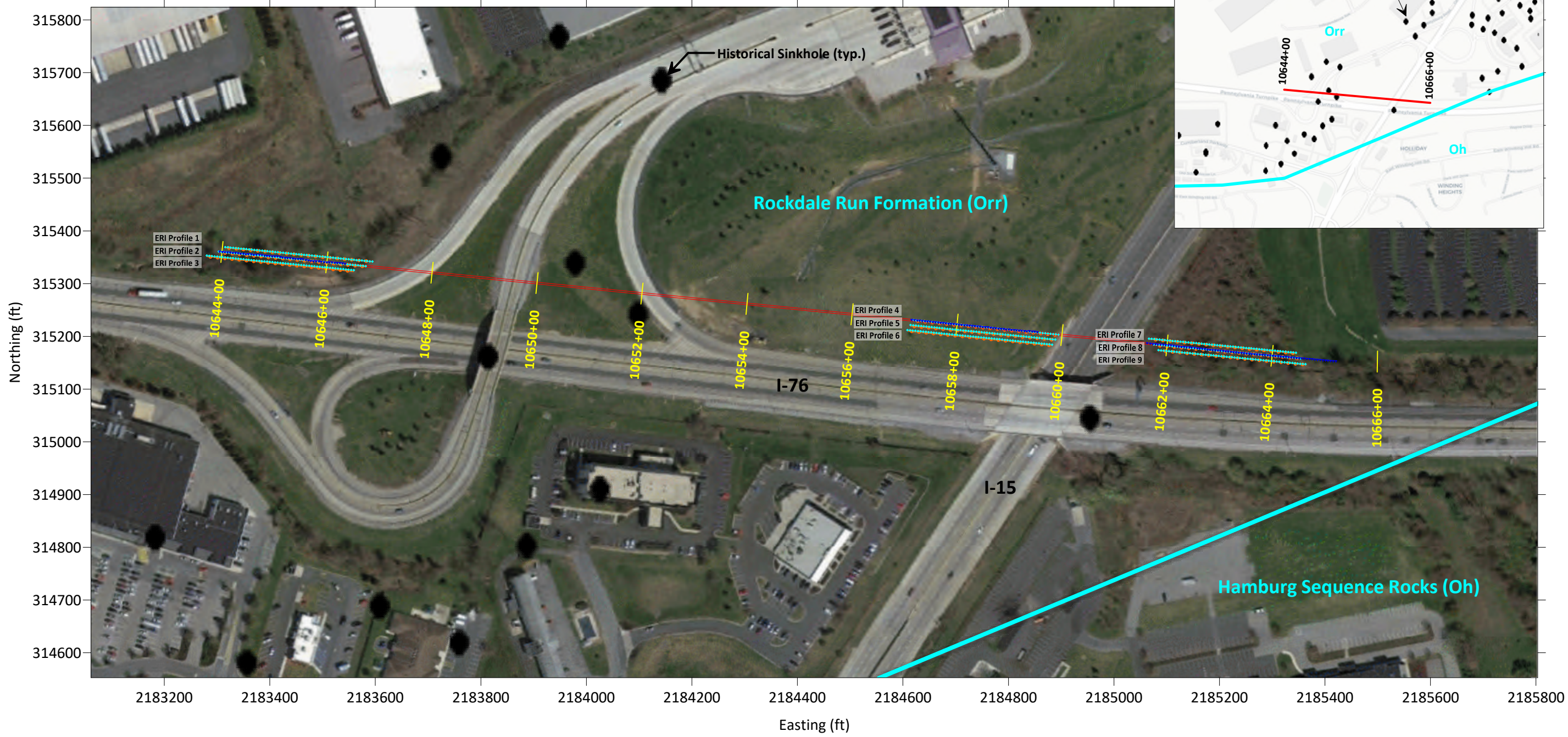
Highway 15  
S2-0247  
PA-CU-0176.0019-RD-16

MIDDLESEX TOWNSHIP  
CUMBERLAND COUNTY, PA



RETTEW Associates, Inc.  
3020 Columbia Avenue, Lancaster, PA 17603  
Phone (717) 394-3721 Fax (717) 394-1063

SURVEY DATE:	11/17/2018
REVIEW NO.:	096302009
REVIEWED BY:	FKB
DRAWN BY:	CHR
DATE:	01/05/2019
SCALE:	1" = 2000'
FIGURE NO.:	1 of 7



SURVEY DATE:	11/17/2018
RETTEW No.:	096302009
REVIEWED BY:	FKB
DRAWN BY:	CHR
DATE:	01/05/2019
SCALE:	1" = 200"
FIGURE NO.:	2 of 7



RETTEW Associates, Inc.  
 3020 Columbia Avenue, Lancaster, PA 17603  
 Phone (717) 394-3721 Fax (717) 394-1063

**Figure 2: Data Coverage Map and Geologic Setting**

Highway 15  
 S2-0247  
 PA-CU-0176.0019-RD-16

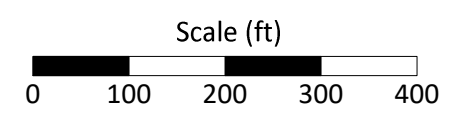
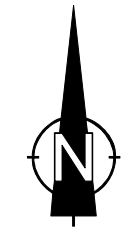
CUMBERLAND COUNTY, PA

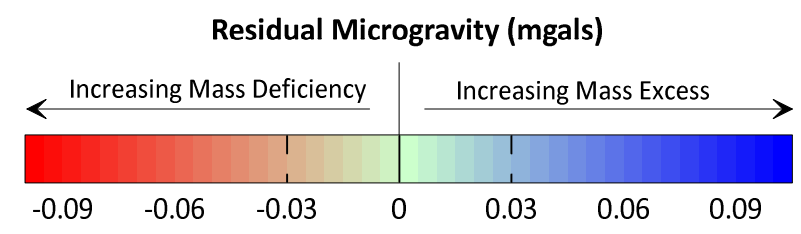
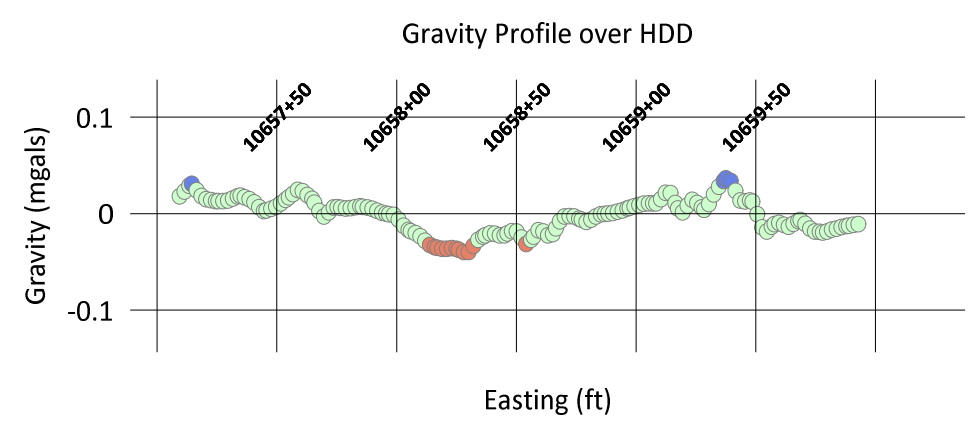
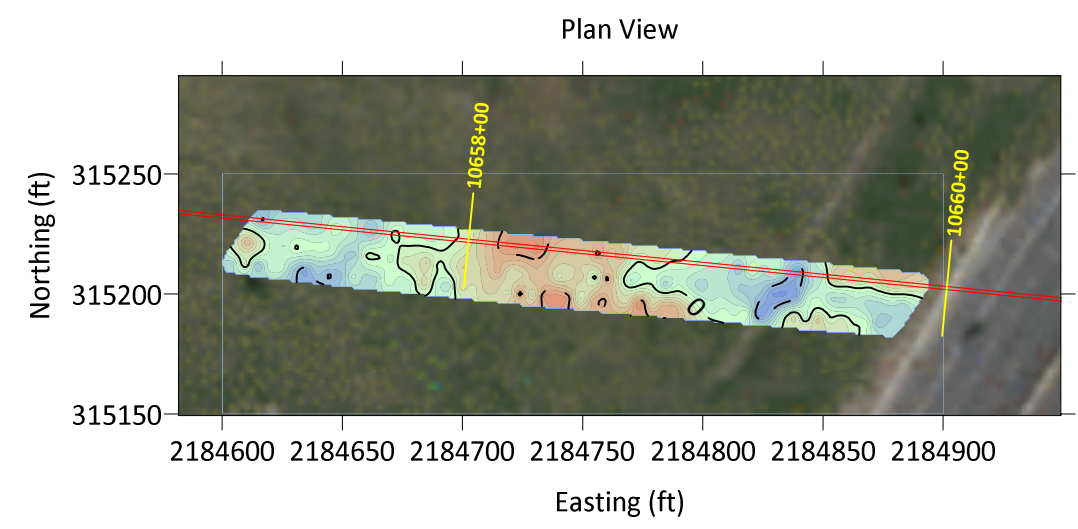
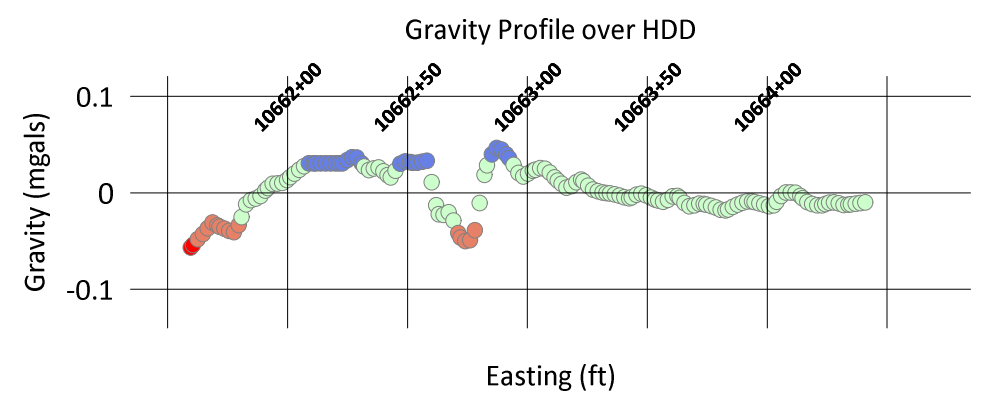
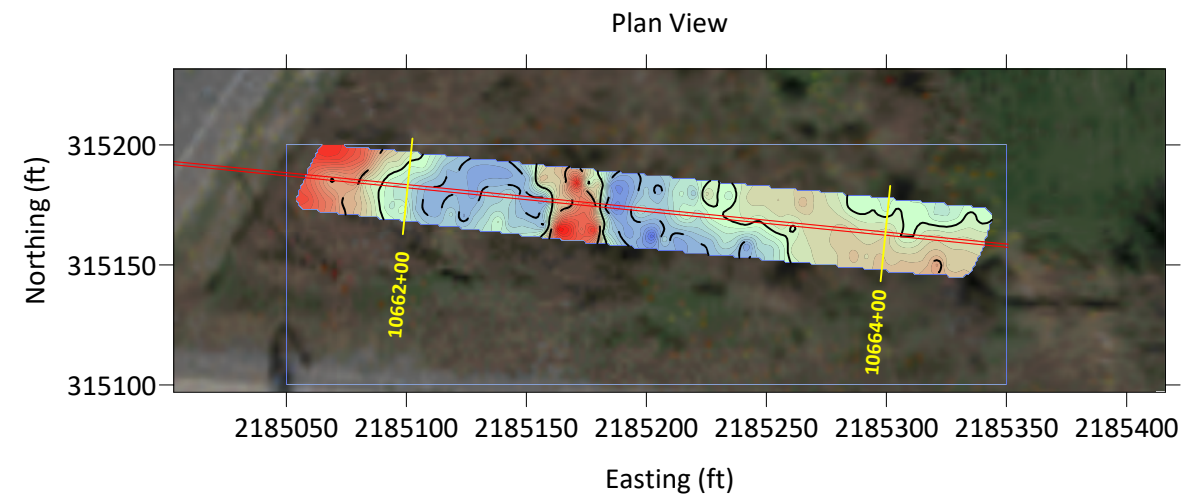
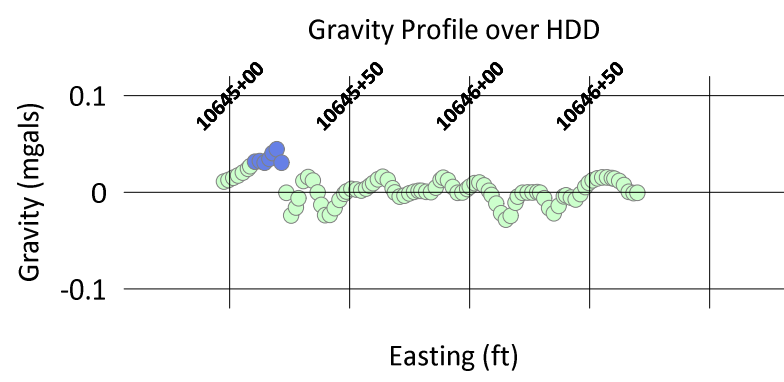
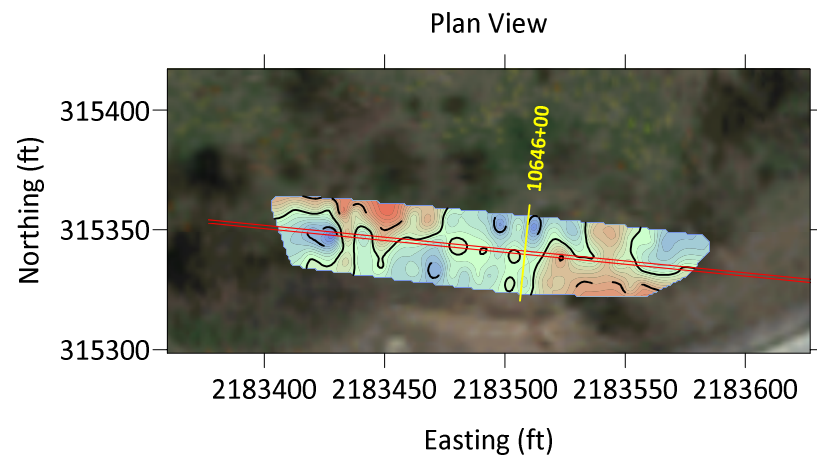
MIDDLESEX TOWNSHIP

Notes:  
 Basemap from Google Earth Pro, extracted 11/2018.  
 Survey profiles/stations from DGPS survey by RETTEW.  
 Geologic information from DCNR WMS Server, extracted 11/2018.

**Geophysical Survey Legend**

- Electrical Resistivity Profile
- Seismic Geophone Location
- Geologic Contact (mapped by others)
- 16" Product Line with Station Number





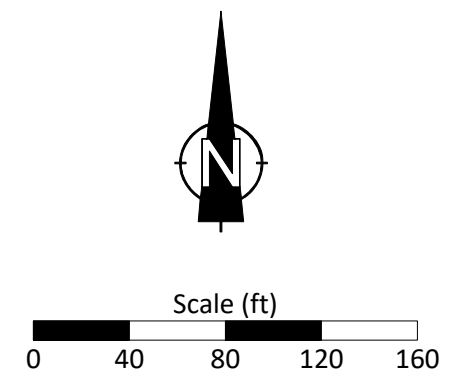
**Geophysical Survey Legend**

11651+00 | 16" Product Line with Station Number

**Notes:**

Basemap from Google Earth Pro, extracted 11/2018.

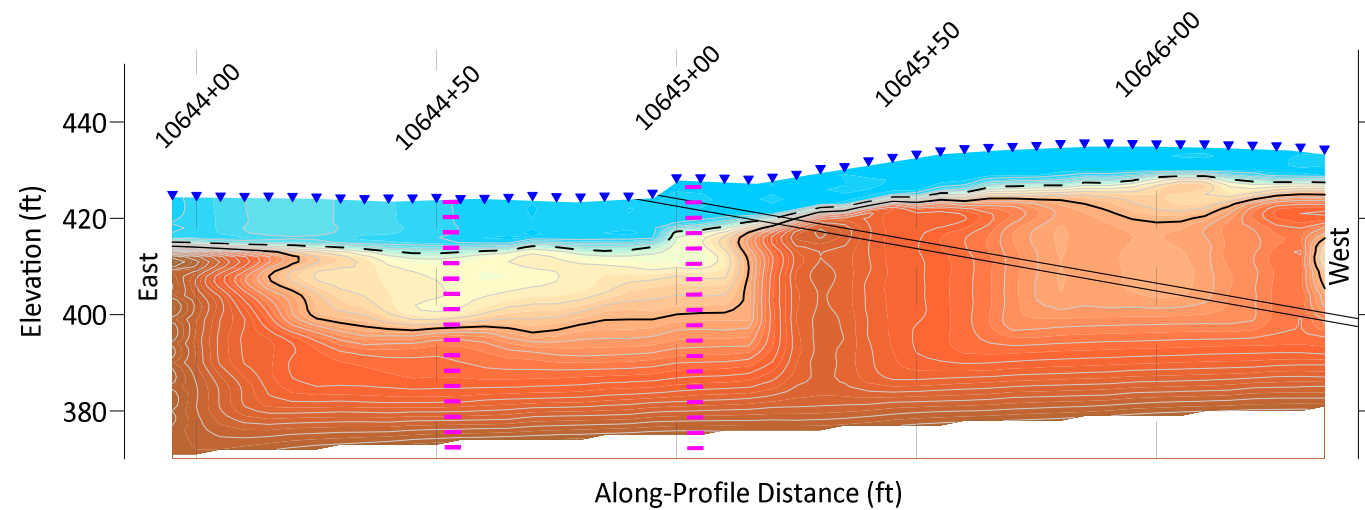
Microgravity data from Scintrex CG-5 gravimeter, with Bouguer correction.



SURVEY DATE:	11/17/2018
RETIEW No.:	096302009
REVIEWED BY:	FKB
DRAWN BY:	CHR
DATE:	01/05/2019
SCALE:	1" = 80'
FIGURE NO.:	3 of 7

**Figure 3: Residual Microgravity Results**

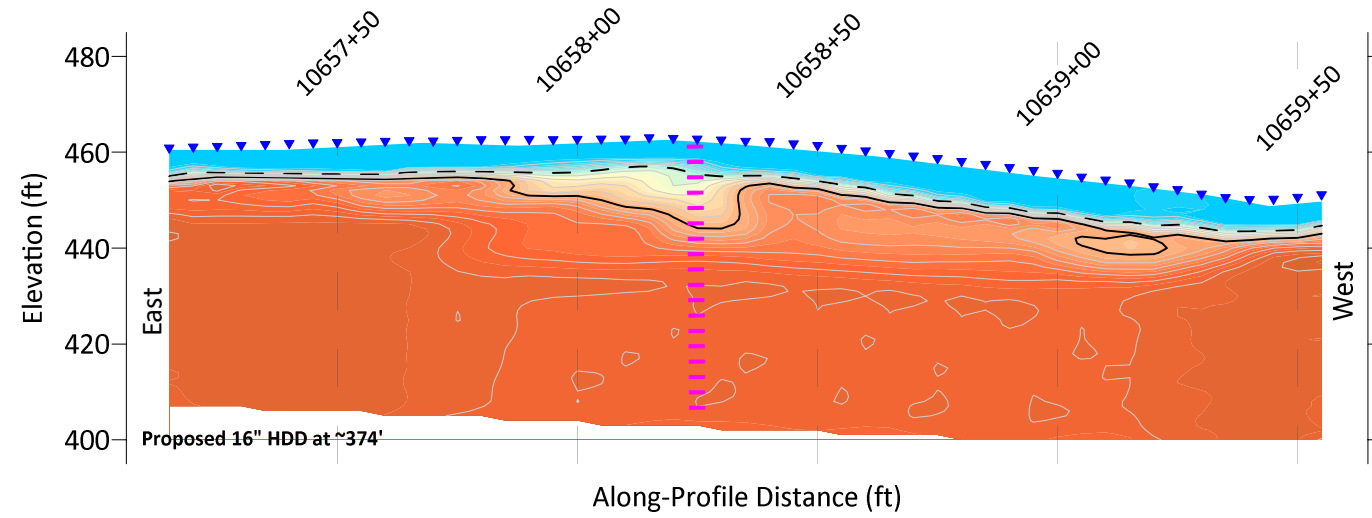
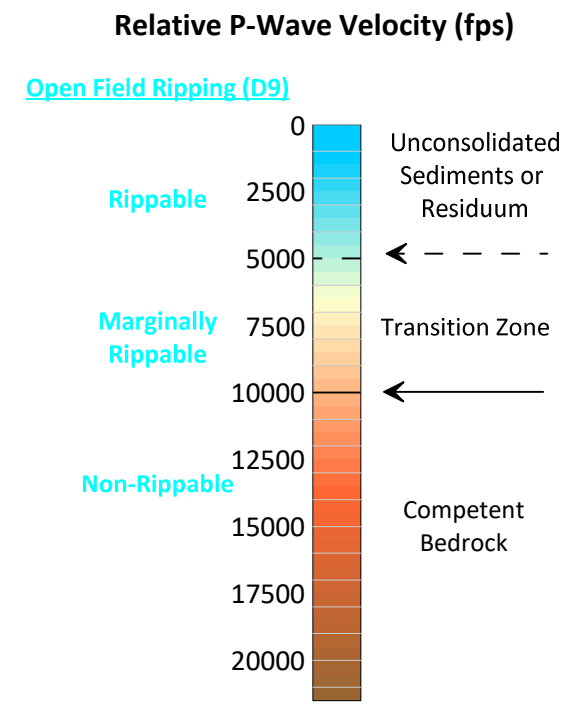
Highway 15  
S2-0247  
PA-CU-0176.0019-RD-16



Weighted Average  
P-Wave Velocity

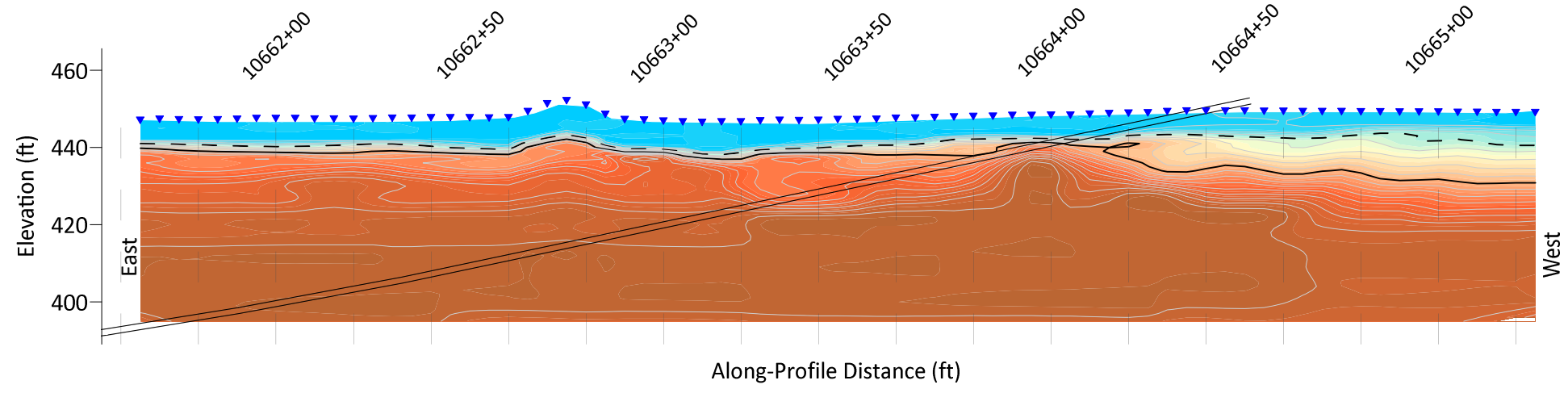
$V_1 = 1,299 \text{ fps}$

$V_2 = 17,172 \text{ fps}$



Proposed 16" HDD at ~374'

- Geophysical Survey Legend**
- ▼ Seismic Geophone Location
  - ▬ Possible Fracture Zone
  - ▬▬ Proposed 16" HDD
  - 11627+00 Station Number



Notes:

Seismic data from Geometrics 24-channel Geode with 4.0 Hz geophones.

Relative seismic velocity models from SeisImager (by Oyo Corporation) tomographic and ray-tracing inversions.

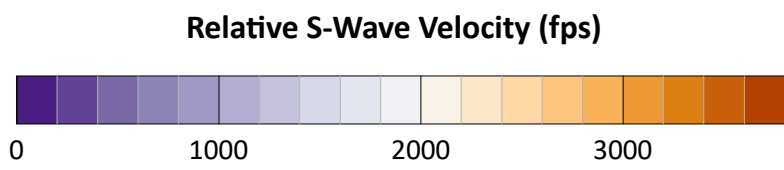
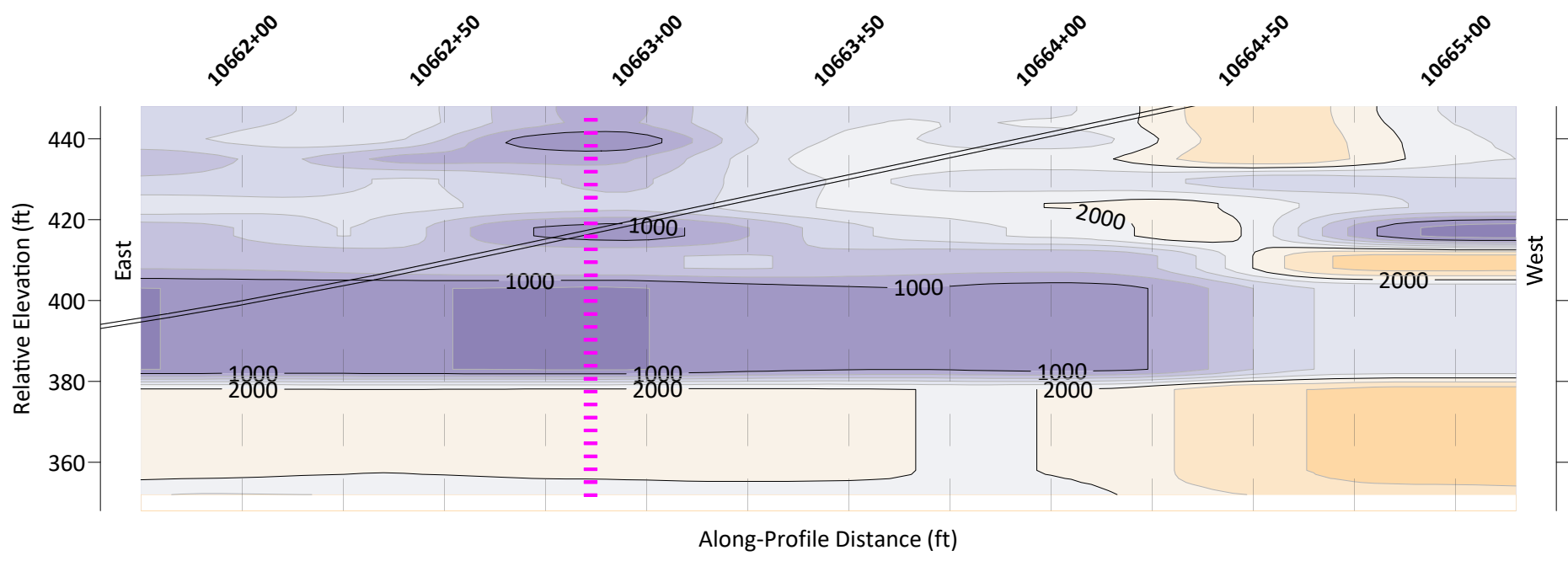
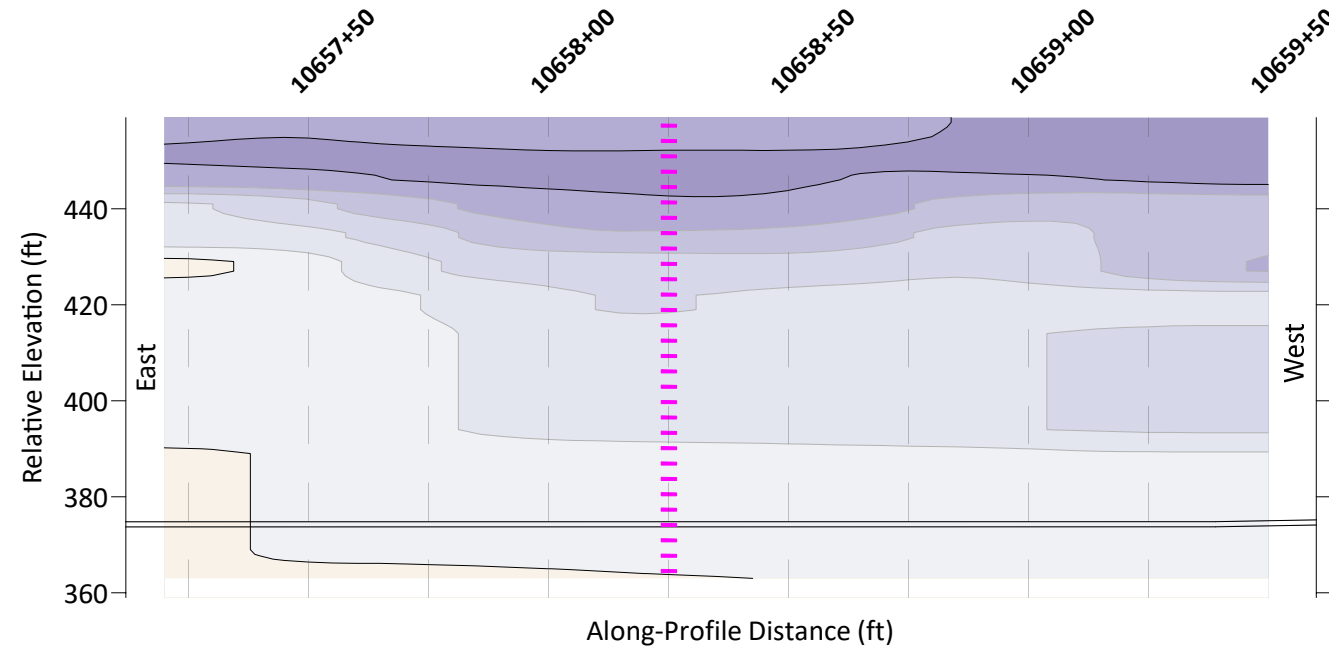
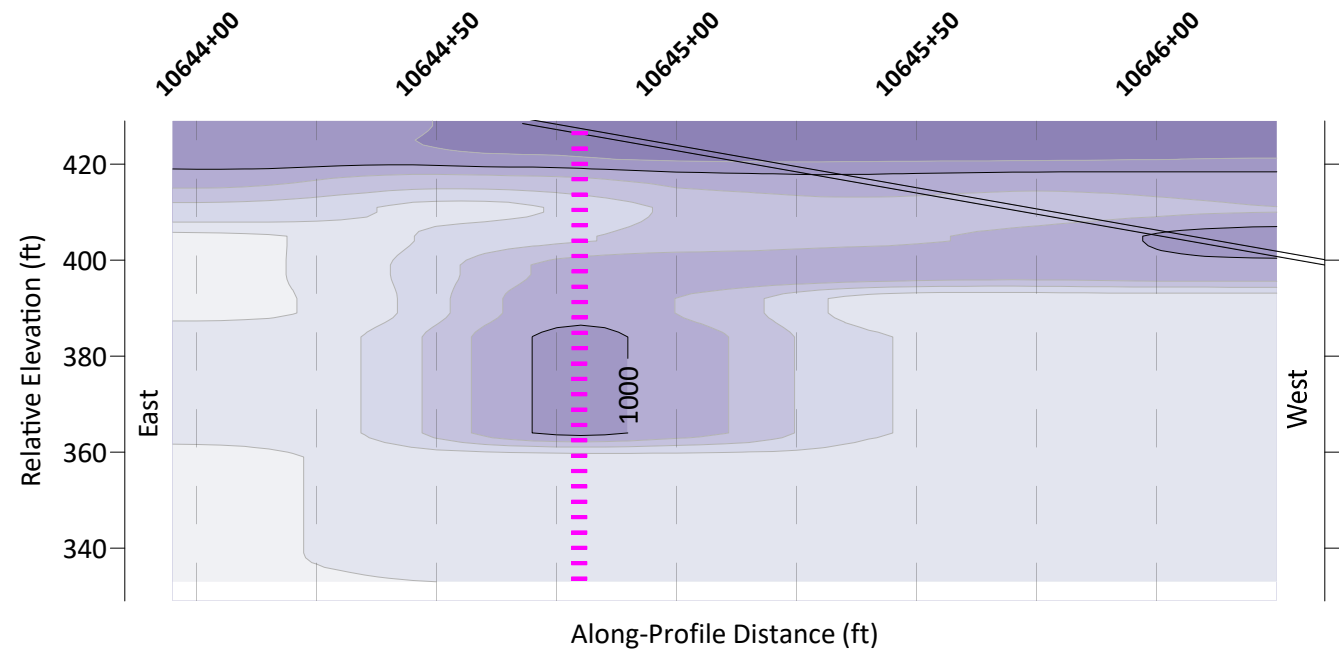
SURVEY DATE:	11/17/2018
RETTEW No.:	096302009
REVIEWED BY:	FKB
DRAWN BY:	CHR
DATE:	01/05/2019
SCALE:	NA
FIGURE NO.:	4 of 7



RETTEW Associates, Inc.  
3020 Columbia Avenue, Lancaster, PA 17603  
Phone (717) 394-3721 Fax (717) 394-1063

**Figure 4: Seismic Refraction Survey Results**

Highway 15  
S2-0247  
PA-CU-0176.0019-RD-16



- Geophysical Survey Legend**
- ▼ Seismic Geophone Location
  - ▬ Possible Fracture Zone
  - ▬▬ Proposed 16" HDD
  - 11627+00 Station Number

Notes:  
 Seismic data from Geometrics 24-channel Geode with 4.0 Hz geophones.  
 Relative seismic velocity models from SeisImager (by Oyo Corporation).

SURVEY DATE:	11/17/2018
RETTEW No.:	096302009
REVIEWED BY:	FKB
DRAWN BY:	CHR
DATE:	01/05/2019
SCALE:	NA
FIGURE NO.:	5 of 7

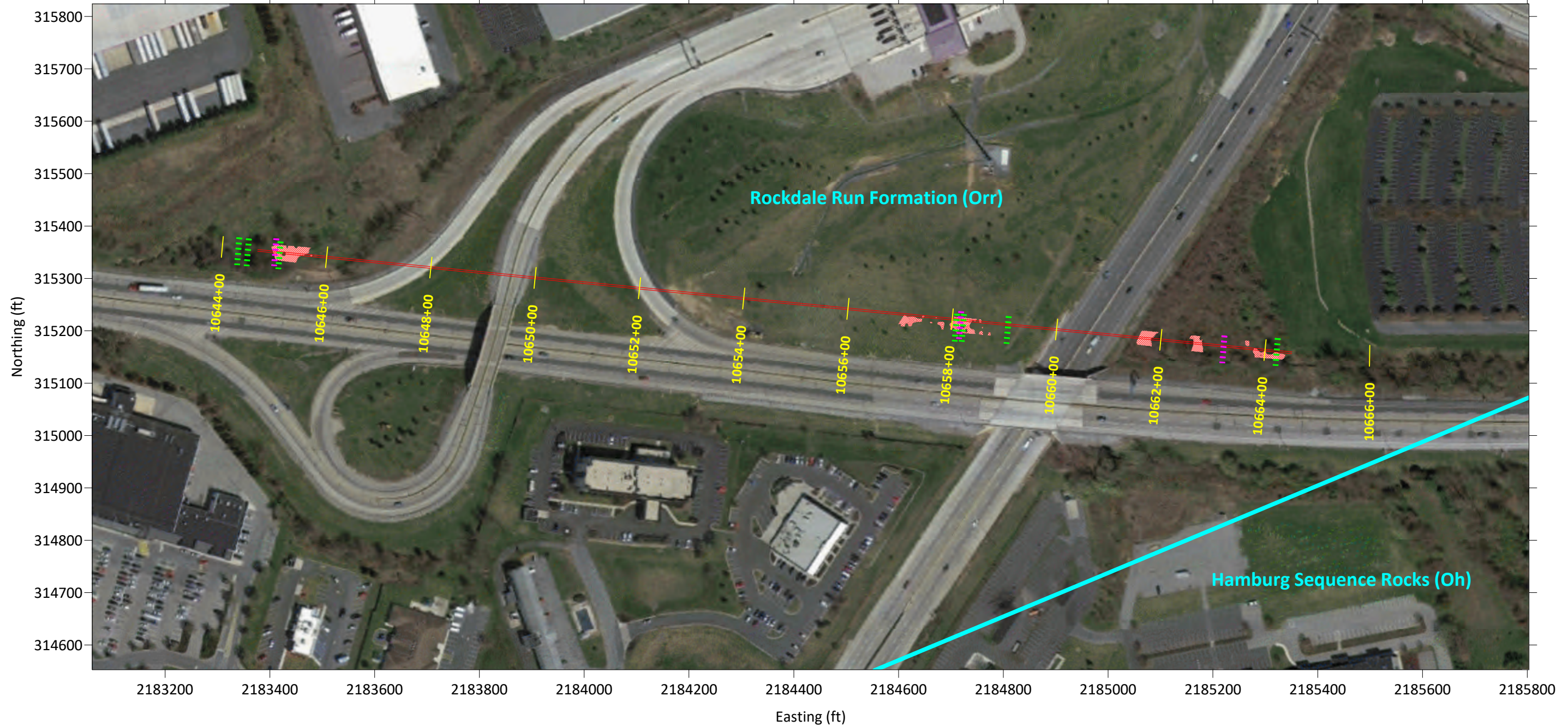


RETTEW Associates, Inc.  
 3020 Columbia Avenue, Lancaster, PA 17603  
 Phone (717) 394-3721 Fax (717) 394-1063

**Figure 5: Seismic MASW Survey Results**

Highway 15  
 S2-0247  
 PA-CU-0176.0019-RD-16





Notes:  
 Basemap from Google Earth Pro, extracted 11/2018.  
 Survey profiles/stations from DGPS survey by RETTEW.  
 Geologic information from DCNR WMS Server, extracted 11/2018.

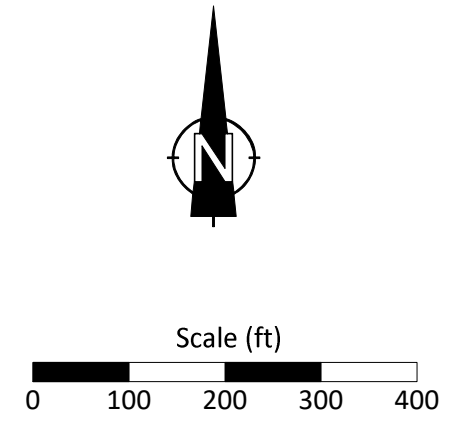
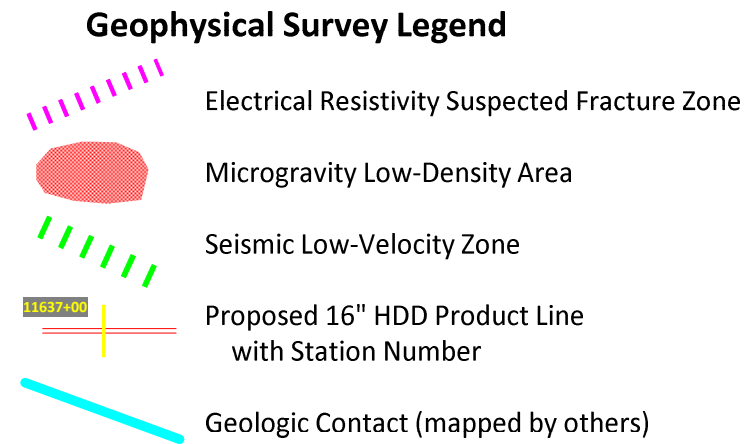


**Figure 7: Geophysical Results Summary**

Highway 15  
 S2-0247  
 PA-CU-0176.0019-RD-16

UPPER ALLEN TOWNSHIP



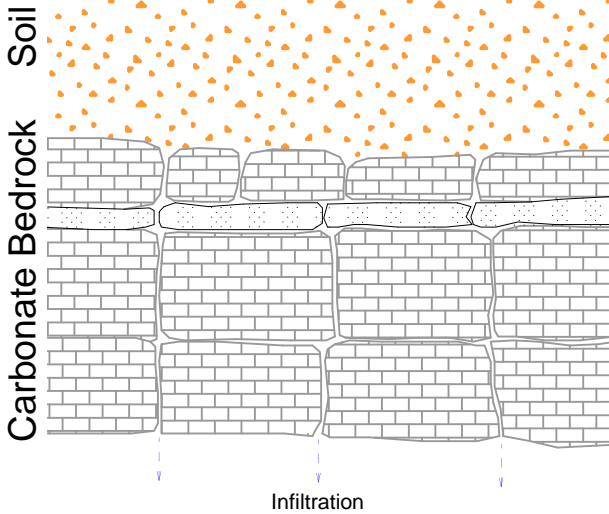
SURVEY DATE:	11/17/2018
RETTEW No.:	096302009
REVIEWED BY:	FKB
DRAWN BY:	CHR
DATE:	01/05/2019
SCALE:	NA
FIGURE NO.:	7 of 7

CUMBERLAND COUNTY, PA

**APPENDIX A**  
*Schematic Karst Processes*

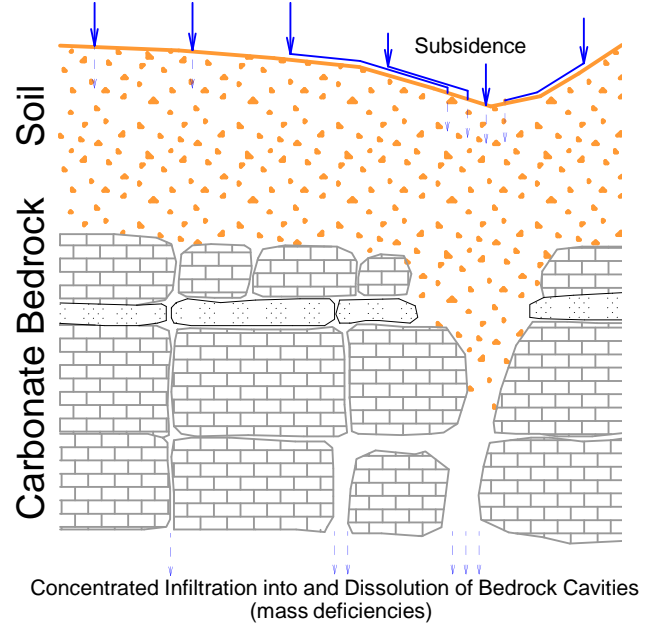
I

Precipitation



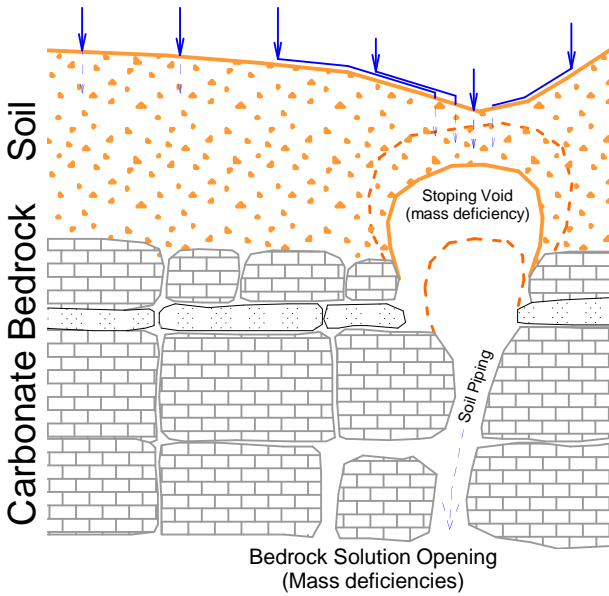
II

Precipitation And Run-Off



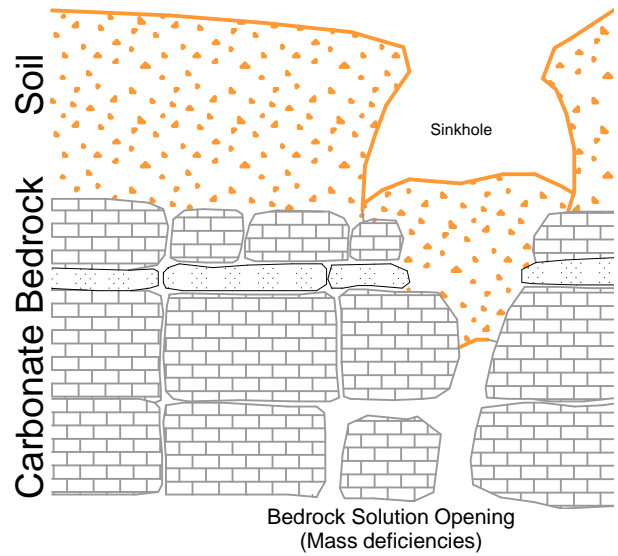
III

Enhanced Precipitation and Run-Off

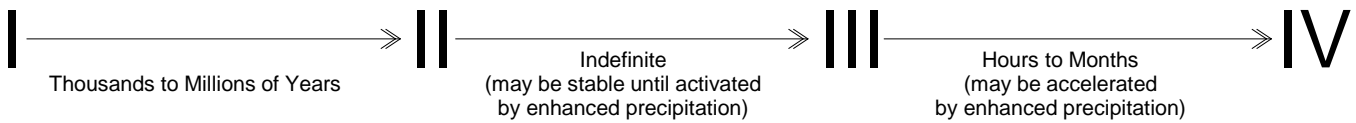


IV

Soil Arch Collapse



### Typical Time Scale



**APPENDIX B**  
*Geophysical Survey Parameters*

### Geophysical Survey Parameters -- I-15

	Spacing <sup>1</sup> (feet)	Shot Interval <sup>2</sup> (feet)	Offset <sup>3</sup> (feet)	Spread Length <sup>4</sup> (feet)	Array Type <sup>5</sup>	Effective Depth <sup>6</sup> (feet)	Lateral Resolution <sup>6</sup> (feet)	Vertical Resolution <sup>6</sup> (percent)	System
Seismic Refraction	5	40	20	120		24	5	15	Geometrics Geode
Seismic MASW	5	5	20	120		40	5	25	Geometrics Geode
ERI	5		20	280	dipole-dipole	75.6	15	variable	AGI Sting R-8
MicroGravity	5		20			size-depth trade-off	depends on depth	depends on depth	Scintrex CG-5

<sup>1</sup> *geophone, electrode, or station*

<sup>2</sup> *Seis (27-lb slidehammer source)*      <sup>3</sup> *distance between parallel profiles*

<sup>4</sup> *ERI or Seis*

<sup>5</sup> *ERI*

<sup>6</sup> *rule-of-thumb only (most depend on site-specific soil properties, sampling interval, depth, and target dimensions)*

**APPENDIX C**  
*Introduction to Seismic Refraction*

## INTRODUCTION TO SEISMIC REFRACTION

BY TIMOTHY D. BECHTEL, PHD, PG

### ENERGY

Mechanical elastic (seismic) waves generated by a hammer blow, weight drop, or explosion.

### SENSITIVITY

Sensitive to elastic properties or moduli – generally strongly correlated with density.

### BASIC EQUIPMENT

Recording Seismograph (generally 24 or more channels); Geophones (one for each channel); Geophone cable; Hammer or weight plus strike plate or explosives; Trigger switch.

### COMMON APPLICATIONS

Determination of the depth and dip of soil horizons and bedrock surfaces. Recent processing advances allow some detection and delineation of discrete targets.

### PRINCIPLES

In a uniform isotropic earth, the shock wave from a blow or explosion at the surface travels outward and downward in a hemispherical wave front like a three-dimensional ripple from a pebble in a still pond. At any point on the wave front, a straight line from the shock source to the wave front depicts the path of the seismic wave and is called a ray path (see **Figure SR-1**). In reality, there are several independent shock waves; the fast-moving primary, compressional or P wave front; the slower moving secondary, shear or S wave (both of which form hemispherical wavefronts); and several disk-like wave fronts that travel only along the surface of the earth (called surface waves or ground roll). For the purposes of most seismic refraction surveys, only the fastest moving wave front — the P wave — is considered. S-wave refraction is used in selected circumstances where complete determination of elastic moduli is desired — particularly when it may be desirable to eliminate the effects of water saturation.

In a layered earth, the hemispherical P shock wave defined by the radially distributed P ray paths are deflected according to the laws of optics (Snell's Law) at interfaces between materials with differing seismic velocities (i.e. densities or elastic properties). Figure SR-2 depicts the deflection of ray paths due to an increase in P velocity at a bedding plane. The type of deflection that a ray path will undergo is dependent upon the angle at which it strikes the interface, and falls into one of four categories:

Some direct rays (green in **Figures SR-2** and **SR-3**) travel parallel to the ground surface at the seismic velocity of the upper layer, do not strike the underlying interface, and consequently are not deflected.

Reflected rays (purple in **Figures SR-2** and **SR-3**) arise where direct rays strike the interface, and a portion of the energy is reflected symmetrically back towards the surface.



The portion of the energy of the incident direct wave that is not reflected upward is refracted or bent as it crosses the interface – making refracted waves in the lower layer (red in **Figures SR-2** and **SR-3**).

At a precise angle called the critical angle, the incident ray is refracted directly along the interface, and travels at the higher seismic velocity of the lower layer (see Critically Refracted Wave in **Figure SR-3**). As this critically refracted or head wave races along beneath the interface, it generates a secondary elastic disturbance that travels back to the surface along ray paths that define a wave front analogous to the bow wake of a ship. These returning rays again travel at the slower velocity of the upper layer.

To perform a refraction survey, a linear array of ground motion sensors or geophones is spaced out from the seismic source or shot point, forming a geophone spread. Each geophone is connected to a separate channel in a seismograph which records a wiggle trace representing the ground motion resulting from the passage of the various seismic rays.

As depicted in the time-distance (T-X) curve in Figure SR-4, the layered earth structure can be determined by analyzing the seismographic wiggle traces. At distances close to the seismic source, the first wiggle or ground motion (the first arrival after the shot) is due to passage of the direct wave travelling at the velocity of the upper layer. Reflected waves arrive later since they have by definition traveled a greater distance at the same velocity (additional later wiggles are caused by passage of the more slowly travelling S and surface waves). Beyond a distance dictated by the critical angle, the first arrival of seismic energy represents the head wave of the critically refracted ray. These refracted rays also by definition travel a greater distance than the direct wave. However, along part of their path, they have traveled at the higher velocity of the underlying more consolidated layer. At greater distances from the shot point, where the path length in the higher velocity layer becomes significant, the head wave arrivals actually race past the direct wave and become the first arrival (see labeled crossover in **Figure SR-4**). By extension, it can be shown that if a third layer with even greater velocity lies at greater depth, the head wave from this layer will become the first arrival at a sufficient distance from the shot point.

In conventional seismic refraction, only the first P wave arrivals can be reliably selected on a wiggle trace record. The later reflected P wave arrivals are generally obscured by the slower-travelling S and surface waves, and the very slow air blast or sound wave from the shot. To interpret a seismic refraction record, the first arrival travel times are measured for each wiggle trace and plotted at the appropriate point on a time-distance (T-X) curve (see Figure SR-4). In a plane-layered earth, these first arrivals define a series of line segments, each representing a discrete layer. The seismic velocity of each layer is simply the reciprocal of the slope of the associated line segment. The thickness of each layer can be calculated from the distances where the line segments intersect. The mathematics for these calculations are easily derived, and can be found in any introductory geophysics text.

True geologic strata are rarely perfectly horizontal. The effect of a dipping interface on a travel time curve cannot be recognized using a single shot point. Calculations based on a T-X curve from a single shot point should always be considered as producing apparent depths to interfaces and apparent seismic velocities for all but the uppermost layer. To determine the true depths and dips of interfaces and the true seismic velocities, it is necessary to reverse the seismic line; that is, move the shot point to a location at or beyond the farthest geophone in the spread, and repeat the shot. The calculation of true depths, dips and velocities from reversed seismic lines is also readily performed.

## CAPABILITIES

Conventional seismic refraction can yield accurate measurements of depths and attitudes of soil horizons, groundwater tables, and other relatively distinct and planar strata. Modern computer analysis of multi-fold seismic refraction data (i.e. with many and overlapping shot points) can provide delineation of undulating or even irregular (as opposed to simply planar) interfaces. The latest generation of computer processing techniques require very high-fold data, but in favorable conditions, are capable of resolving even discrete targets such as foundation elements, tunnels or cavities, and can resolve gradational boundaries as well as distinct interfaces. The seismic P-wave velocities of materials are generally an indication of relative density or compaction. S-wave refraction data (collected using specialized geophones, shock sources and field procedures) can provide S-wave velocities that bear a well-constrained empirical relationship to standard penetration test (SPT) N values and therefore bearing capacity. For surveys where matching P- and S-wave velocities are determined, the dynamic elastic moduli of subsurface materials can be calculated (including Poisson's Ration, Young's or Bulk Modulus, and Shear Modulus or Rigidity).

## LIMITATIONS

Seismic data is collected at spaced geophones, and therefore does not provide continuous profile data. If geophones are spaced too widely, thin layers can be missed entirely.

Conventional refraction interpretations are only accurate where the velocity of strata increase with depth. Velocity inversions not only alter the data, but are particularly insidious since the presence of a low velocity zone at depth is not apparent in first arrival data. The latest generation of computer processing techniques do allow detection and delineation of laterally restricted low velocity zones (e.g. tunnels, cavities, gravel lenses, etc.).

Sharp or dramatic interface relief such as limestone pinnacles cannot always be resolved even with very tight geophone spacing. Therefore, refraction profiles of expectedly irregular interfaces should be assumed to represent somewhat smoothed versions of actual relief (see e.g. Figure **SR-5**).

Seismic records can contain noise due to heavy machinery vibrations, vehicular traffic, and sometimes even wind or distant earthquakes. Care must be taken to identify potential sources of seismic noise prior to beginning a survey.

The effective survey depth is limited to approximately 1/5 of the greatest shotpoint to geophone distance. Therefore, very deep surveys may require impractically long lines (requiring consideration of other geophysical techniques such as seismic reflection).

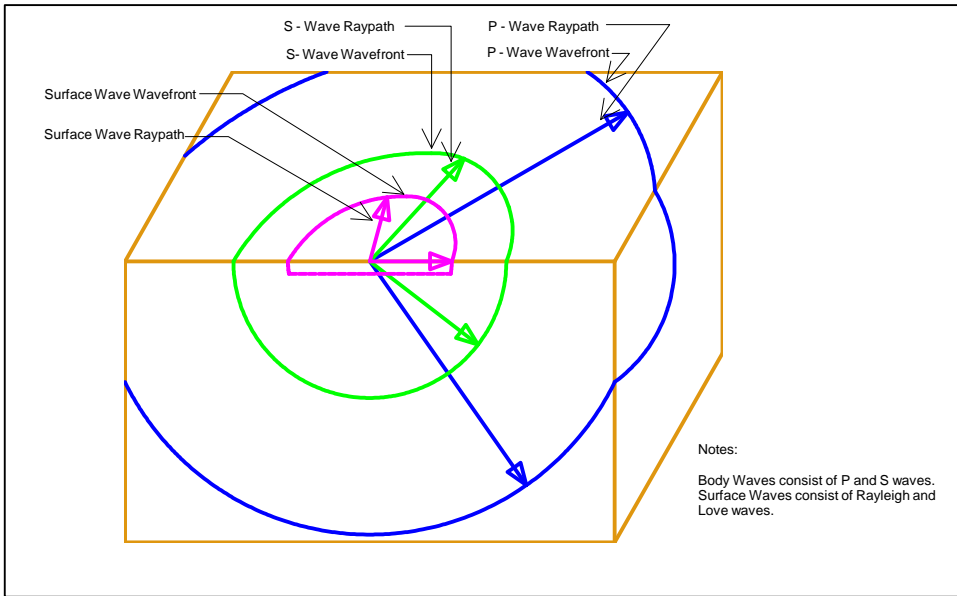


Figure SR-1

Seismic Wave Types

Rev. 04/2018

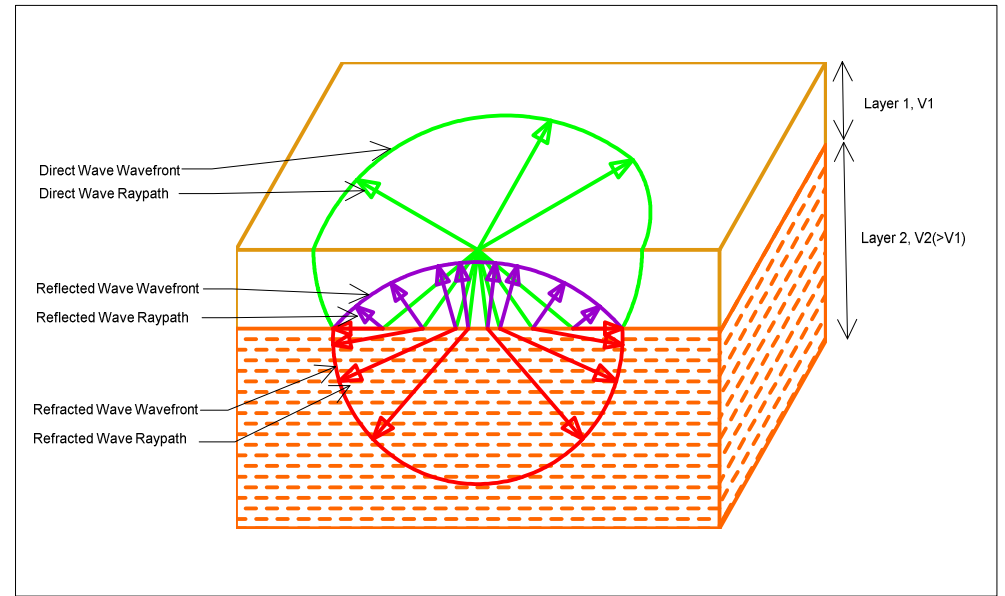


Figure SR-2

Effect of Layering  
on Body Wave Raypath

Rev. 04/2018

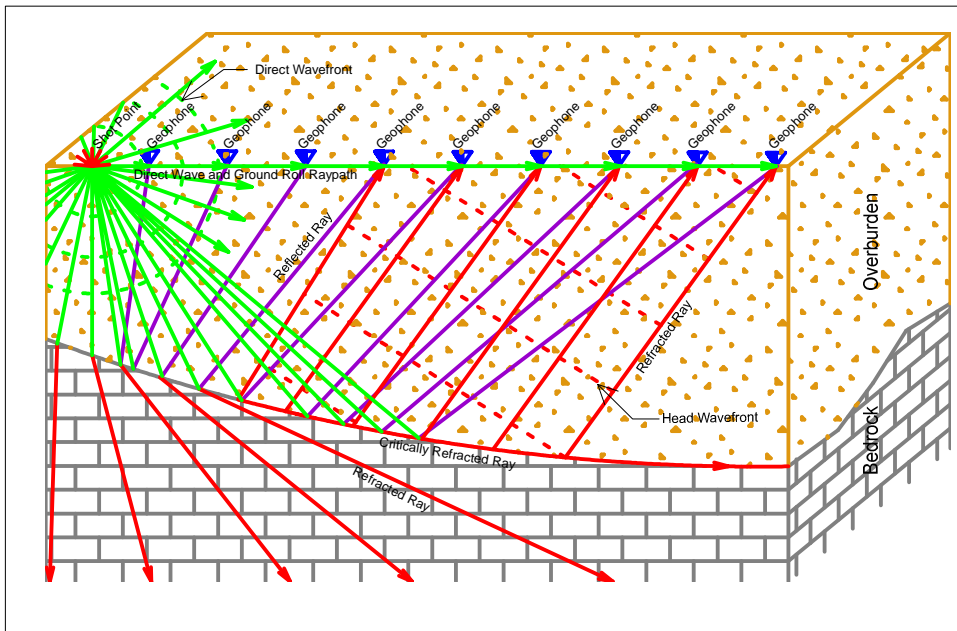


Figure SR-3

Seismic Ray Path Geometry

Rev. 04/2018

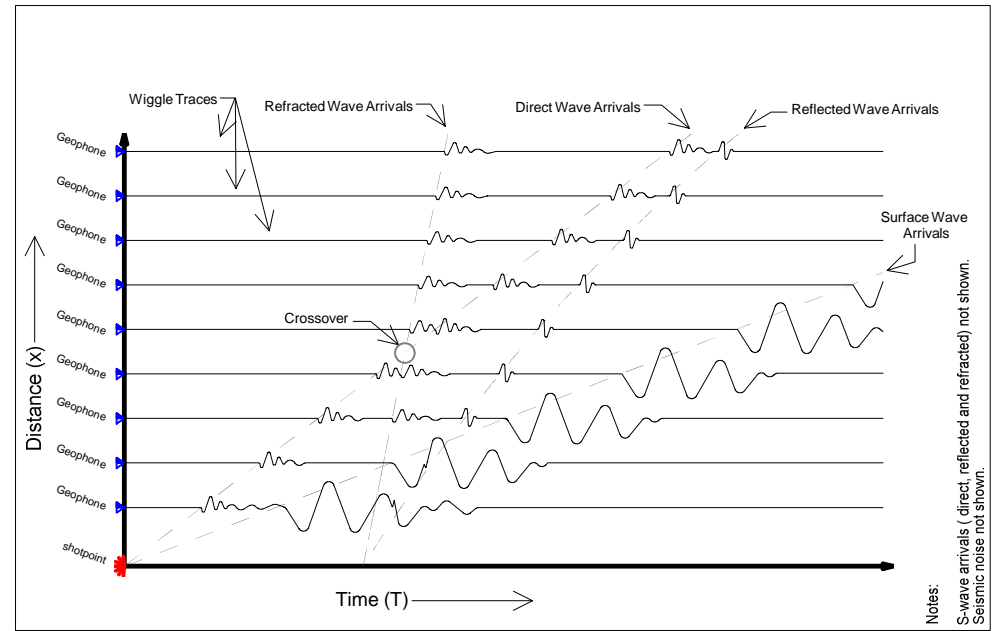
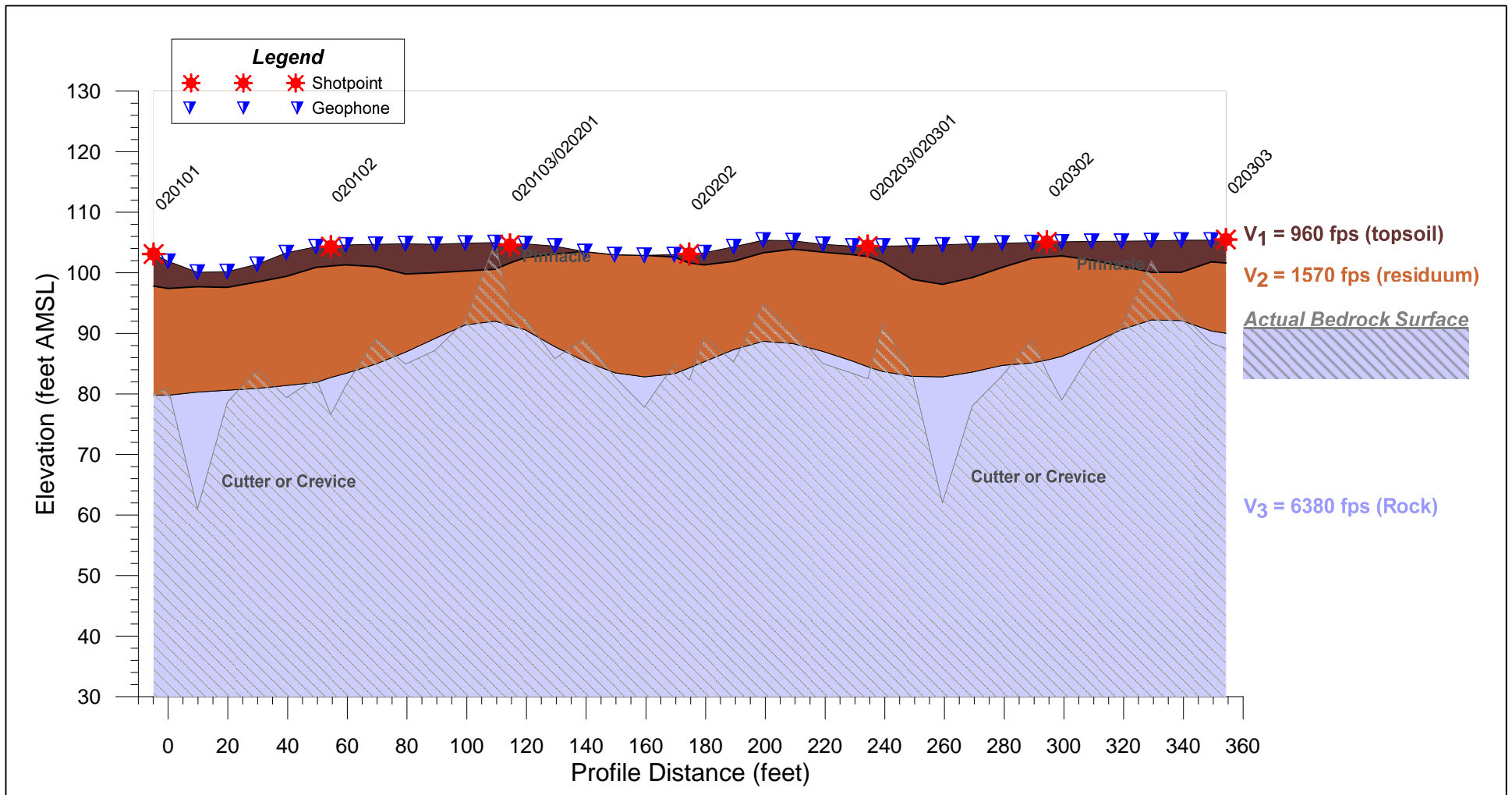


Figure SR-4

Idealized  
Seismic Record  
and T- X Graph

Rev. 04/2018





**Figure SR-5**

**Example Karst Terrane Seismic Profile**

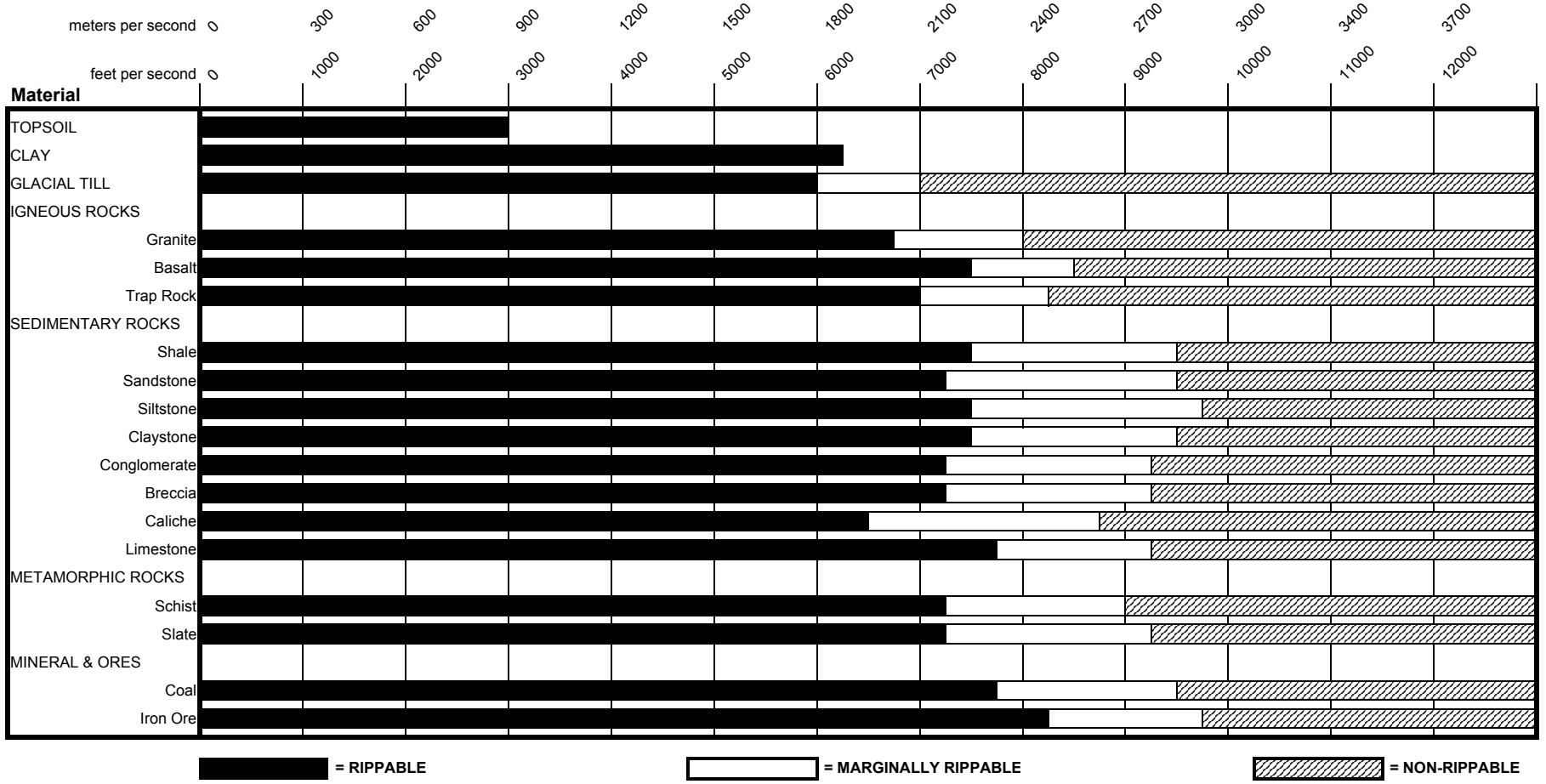
Revised 04/2018



**APPENDIX D**  
*Caterpillar Ripping Charts*

**Ripping Chart \***  
**D9R**  
 Multi or Single Shank No. 9 Ripper  
 Estimated by Seismic P-Wave Velocities

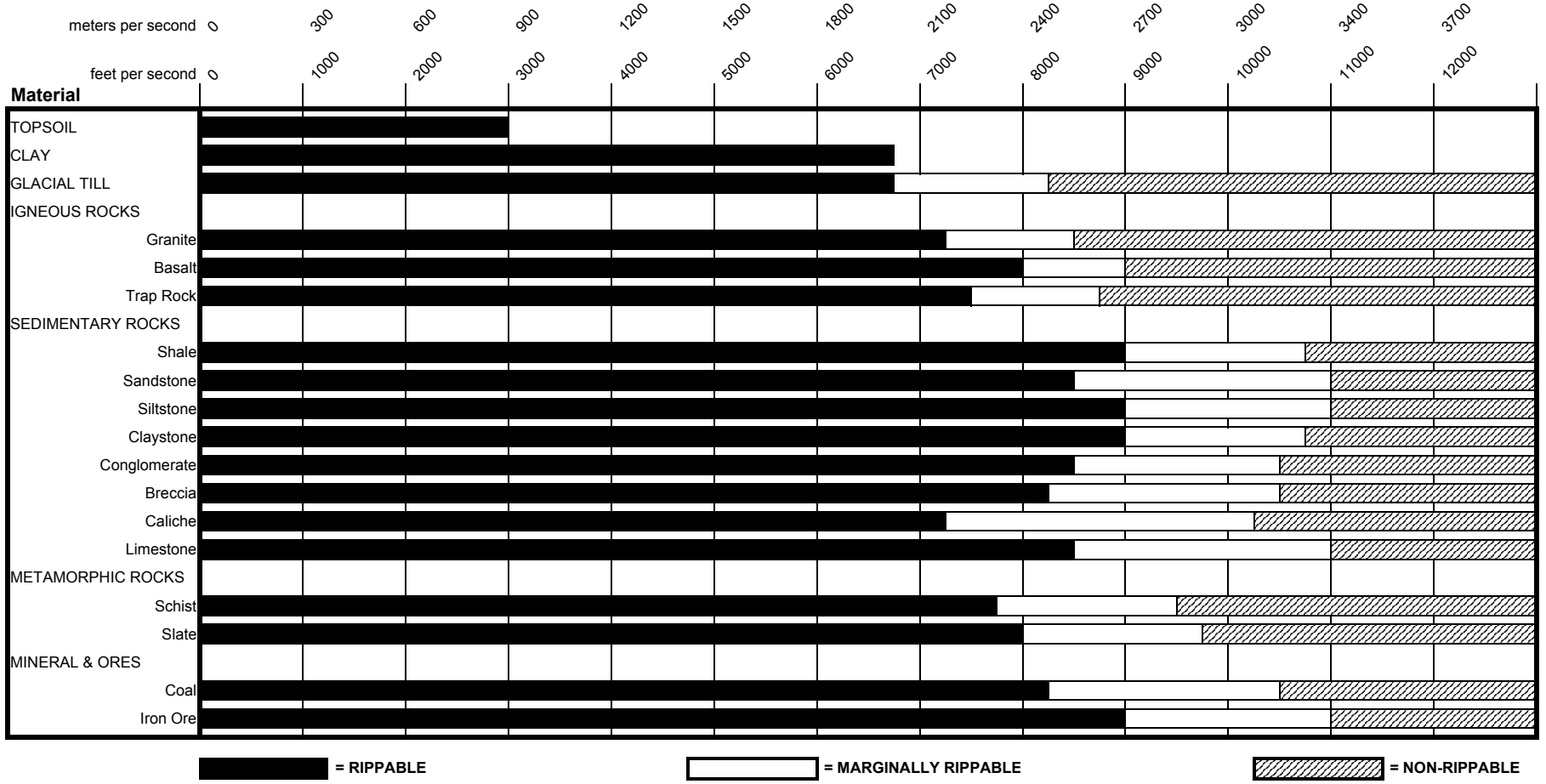
**Seismic Velocity**



\* Caterpillar Performance Handbook, Edition 26, Caterpillar, Inc., Peoria, Illinois

**Ripping Chart \***  
**D10N**  
 Multi or Single Shank No. 10 Ripper  
 Estimated by Seismic P-Wave Velocities

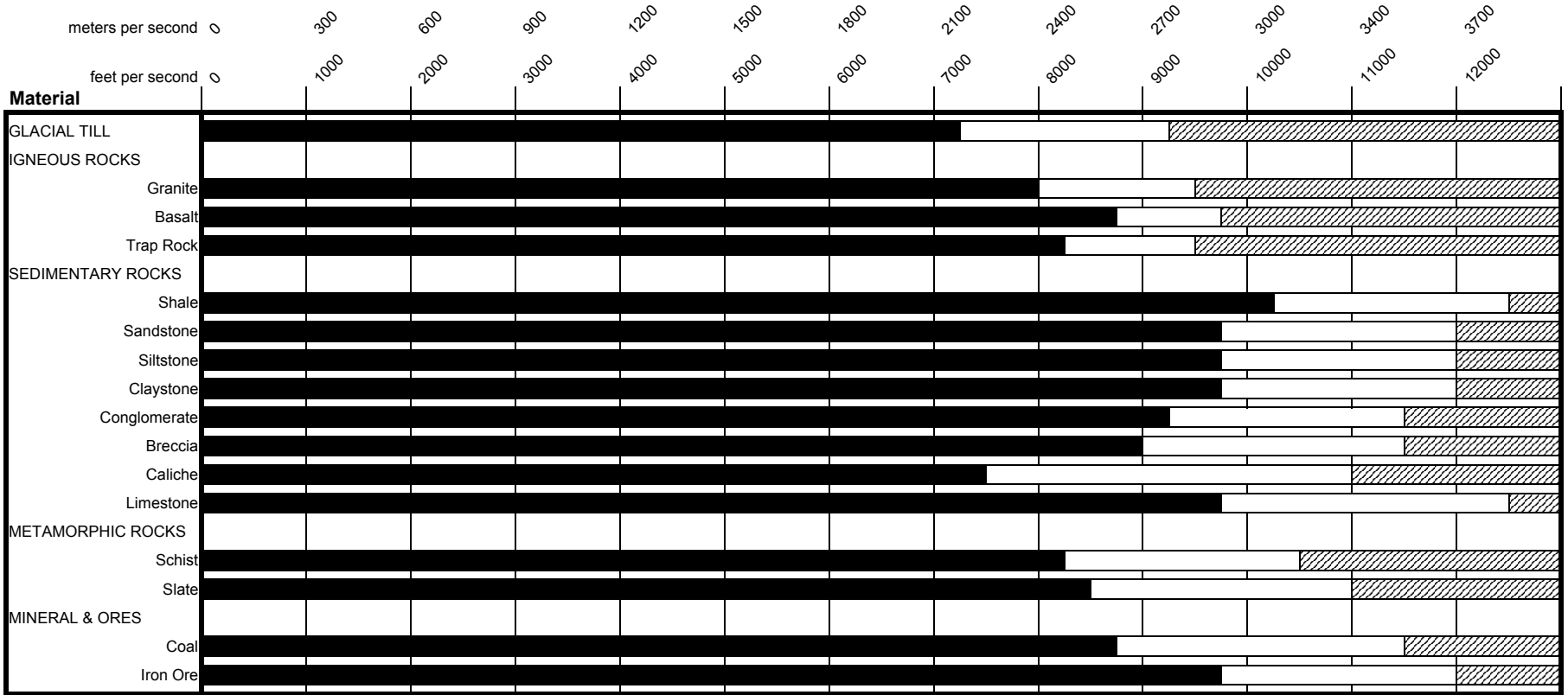
**Seismic Velocity**



\* Caterpillar Performance Handbook, Edition 26, Caterpillar, Inc., Peoria, Illinois

**Ripping Chart \***  
**D11N**  
**Multi or Single Shank No. 11 Ripper**  
**Estimated by Seismic P-Wave Velocities**

**Seismic Velocity**



= RIPPABLE

= MARGINALLY RIPPABLE

= NON-RIPPABLE

\* Caterpillar Performance Handbook, Edition 26, Caterpillar, Inc., Peoria, Illinois